

X-Mark: Saliency-Guided Robust Dataset Ownership Verification for Medical Imaging

Pranav Kulkarni, Junfeng Guo and Heng Huang

University of Maryland Institute for Health Computing, North Bethesda, MD
 {pranavk, gjf2023, heng}@umd.edu,

Abstract

High-quality medical imaging datasets are essential for training deep learning models, but their unauthorized use raises serious copyright and ethical concerns. Medical imaging presents a unique challenge for existing dataset ownership verification methods designed for natural images, as static watermark patterns generated in fixed-scale images scale poorly dynamic and high-resolution scans with limited visual diversity and subtle anatomical structures, while preserving diagnostic quality. In this paper, we propose X-Mark, a sample-specific clean-label watermarking method for chest x-ray copyright protection. Specifically, X-Mark uses a conditional U-Net to generate unique perturbations within salient regions of each sample. We design a multi-component training objective to ensure watermark efficacy, robustness against dynamic scaling processes while preserving diagnostic quality and visual-distinguishability. We incorporate Laplacian regularization into our training objective to penalize high-frequency perturbations and achieve watermark scale-invariance. Ownership verification is performed in a black-box setting to detect characteristic behaviors in suspicious models. Extensive experiments on CheXpert verify the effectiveness of X-Mark, achieving WSR of 100% and reducing probability of false positives in Ind-M scenario by 12%, while demonstrating resistance to potential adaptive attacks.

1 Introduction

The release of large-scale, high-quality medical imaging datasets has advanced the utility of deep learning (DL) models in clinical settings, demonstrating its potential across diagnosis, prognosis, and treatment planning [Rajpurkar and Lungren, 2023]. Curating such datasets is a substantial investment, both time-consuming and expensive, especially when expert annotations from radiologists are required [Diaz-Pinto *et al.*, 2024; Ma *et al.*, 2024]. The value of these high-quality datasets is further amplified as radiology AI tools are rapidly commercialized and cleared by the FDA [Ebrahimian *et al.*, 2022]. This raises concerns regarding the unauthorized

commercial use of public datasets released solely for research purposes.

Consider the MIMIC dataset, a large publicly accessible collection of chest x-rays (CXRs), radiology reports, and electronic health record [Johnson *et al.*, 2019; Johnson *et al.*, 2023]. It represents a high-value resource for research, requiring a data use agreement and credentialing process involving HIPAA training. Despite these safeguards, the dataset remains susceptible to unauthorized commercial use if distributed outside of approved channels. Such misuse is not only a serious violation of the dataset owners' intellectual property, but also presents significant ethical concerns regarding patient privacy.

While several groups have explored dataset copyright protection for DL models, they are primarily designed for natural images, and methods intended for medical imaging remain relatively underexplored [Abadi *et al.*, 2016; Hua *et al.*, 2023]. Dataset ownership verification (DOV) is the most common and effective strategy, relying on the embedding of watermarks into a small subset of samples within the released dataset [Li *et al.*, 2022; Li *et al.*, 2023]. Any model trained on this watermarked dataset learns the association between the watermark and specific labels, allowing the dataset owner to detect unauthorized use even in a black-box setting.

In this work, we focus on CXRs which present two challenges for existing DOV methods. First, previous methods rely on fixed-size static backdoor patterns, which scale poorly to the dynamic and high-resolution scans typically encountered with CXRs (e.g., often exceeding 2000×2500). Since DL models are trained on downsampled versions of these images, watermarks must remain effective even after resizing. Second, CXRs exhibit limited visual diversity and subtle anatomical structures in grayscale, requiring watermarks to be embedded within a single-channel while preserving diagnostic quality. This constraint makes watermark effectiveness and imperceptibility especially challenging: If the perturbation is too strong, watermarks may become easy to detect upon manual inspection. High-frequency perturbations that are imperceptible may not survive downsampling, while perturbations that blend with the image characteristics may inadvertently trigger benign models. Together, these challenges limit the effectiveness of DOV methods in medical imaging.

To address these limitations, we propose X-Mark, a sample-specific clean-label backdoor watermarking method

for CXR copyright protection. Our method uses a U-Net with an EigenCAM-based saliency conditioning module that generates unique perturbations within salient regions of each sample. We design a multi-component training objective to ensure watermark efficacy, robustness against dynamic scaling processes, while preserving diagnostic quality and visually-distinguishability. We incorporate Laplacian regularization [Denton *et al.*, 2015] into our training objective to penalize high-frequency perturbations and achieve watermark scale-invariance. Extensive experiments on CheXpert [Irvin *et al.*, 2019] verify the effectiveness of X-Mark, achieving WSR of 100% and reducing probability of false positives in Ind-M scenario by 12%, while demonstrating resistance to potential adaptive attacks. Our main contributions are three-fold:

- We propose a sample-specific clean-label backdoor watermarking method for medical image copyright protection. Our method uses a conditional U-Net to generate unique perturbations within salient regions, addressing the limitations of existing DOV methods designed for natural images when extended to medical imaging.
- We introduce Laplacian regularization in the watermark generator to penalize high-frequency perturbations, encouraging the model to produce perturbations that are robust to downsampling.
- We perform extensive experiments on CXRs to demonstrate watermark effectiveness, imperceptibility, and transferability.

2 Related Work

Medical Data Protection The rapid expansion of artificial intelligence in healthcare has raised significant concerns regarding unauthorized exploitation of medical datasets [Sembekov *et al.*, 2020]. To address these concerns, medical image watermarking techniques have been developed to embed ownership information directly into medical images using methods such as discrete wavelet transform (DWT) and device fingerprinting [Poonam and Arora, 2022; Kancharla and others, 2024]. However, traditional watermarking may not be suitable for dataset ownership verification since embedded watermarks can hardly be inherited by trained models. More recently, Sun et al. [Sun and others, 2024] proposed the Sparsity-Aware Local Masking (SALM) method, which generates unlearnable examples specifically designed for medical data by selectively perturbing significant pixel regions, leveraging the inherent sparse nature of medical images while maintaining clinical utility. However, similar to other unlearnable example methods [Huang *et al.*, 2021], Sun et al. requires watermarking over 90% of the training data to ensure efficacy, which would limit its practical applicability.

Data Ownership Protection (Auditing) with Watermark Dataset Ownership Verification (DOV) has emerged as a promising solution to protect dataset copyrights in deep learning [Li *et al.*, 2023; Maini *et al.*, 2021]. Existing DOV methods can be categorized into two main types based on their reliance on internal features (IF) versus external features (EF) [Shao *et al.*, 2025]. IF-based methods exploit inherent

data characteristics such as model overfitting through membership inference [Maini *et al.*, 2021]. EF-based methods introduce artificial features into datasets, primarily through backdoor watermarking [Adi *et al.*, 2018; Li *et al.*, 2022; Tang *et al.*, 2023] that induces identifiable model behaviors, or non-poisoning watermarks [Sablayrolles *et al.*, 2020; Guo *et al.*, 2024] that embed features without causing misclassification. For unlabeled data, watermarking has been extended to self-supervised learning scenarios to protect pre-trained encoders [Wu *et al.*, 2022; Cong *et al.*, 2022]. However, recent adversarial evaluations [Zhu *et al.*, 2025; Shao *et al.*, 2025] have revealed that current DOV methods remain vulnerable to evasion attacks, underscoring the need for more robust dataset auditing approaches.

3 Conditional Scale-Invariant Clean-label Backdoor Watermark

3.1 Preliminaries

Threat model We focus on dataset ownership verification with watermark in medical image classification. There are two parties involved: a dataset owner and an unauthorized user. The dataset owners release their dataset for research or other innocent purposes, while protecting its copyright and preventing unauthorized use. The unauthorized user has incentive to train their commercial model without permission from the dataset owner. If the owner finds a suspicious model, unauthorized use of watermarked dataset can be verified by detecting characteristic behaviors in a black-box setting.

Main Pipeline of Dataset Watermarking Consider a benign dataset $\mathcal{D} = \{(\mathbf{x}_i, \mathbf{y}_i)\}_{i=1}^N$ containing N samples. Each sample includes a medical image $\mathbf{x}_i \in \mathbb{R}^{H \times W}$ and its labels $\mathbf{y}_i \in \{0, 1\}^K$. Specifically, this formulation describes a multi-label setting, where each $\mathbf{y}^{(k)}$ is a binary label for which $\mathbf{y}_i^{(k)} = 1$ indicates the presence of k -th pathology and vice versa. In contrast to multi-class settings, each sample may contain multiple pathologies.

The dataset owner selects a subset $\mathcal{D}_s \subset \mathcal{D}$ of samples from their dataset with watermarking rate γ . Generally, these samples share the same target label y_t defined under a multi-class setting as $y_t \in \{1, 2, \dots, K\}$. This formulation can be extended to the multi-label setting by selecting a specific target label $y^{(k)}$. Here, the target and non-target classes are defined as $y_t^{(k)} = 1$ and $y_{nt}^{(k)} = 0$ respectively. For each sample $\mathbf{x}_i \in \mathcal{D}_s$, its watermarked version $\hat{\mathbf{x}}_i = G(\mathbf{x}_i; \theta)$ is generated using a watermark generator. This set of watermarked samples \mathcal{D}_p is then combined with the remaining dataset $\mathcal{D} \setminus \mathcal{D}_s$ to create the watermarked dataset \mathcal{D}_w , and is subsequently released for legitimate use.

Consider a suspicious model in a black-box setting, where the owner only has access to the model’s API. The dataset owner intends to determine whether this model was trained on the watermarked dataset \mathcal{D}_w . A hypothesis-test-guided method based on the model’s predicted probabilities on watermarked verification samples generated by $G(\cdot; \theta)$ are used to determine unauthorized use of dataset. Specifically, this looks for characteristic backdoor behaviors where the sus-

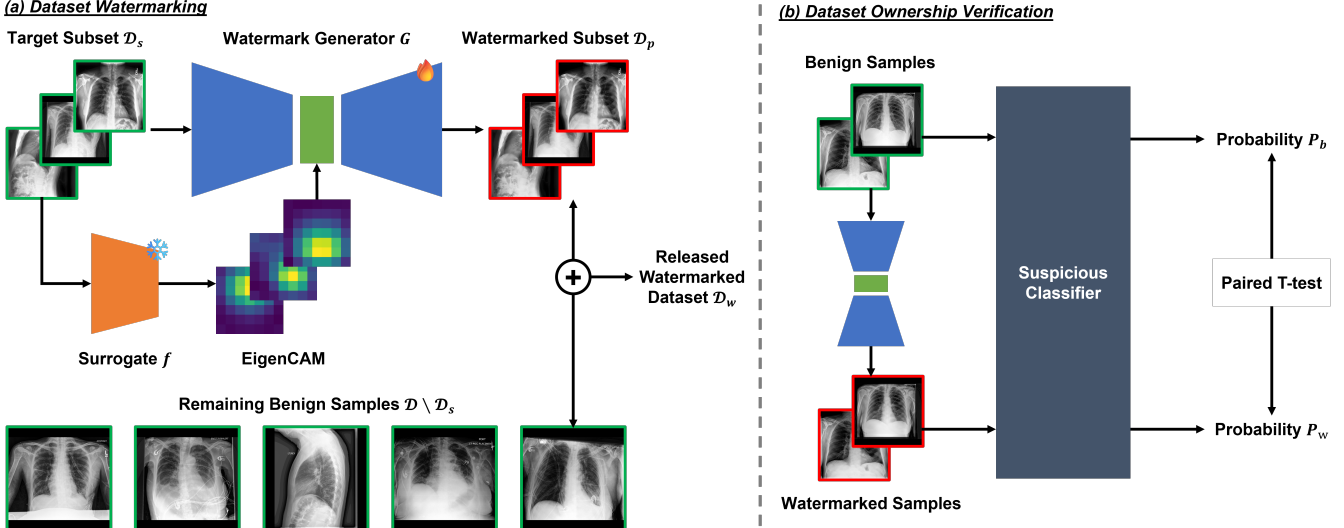


Figure 1: The main pipeline of X-Mark. First, a conditional U-Net is trained to generate sample-specific watermarks within salient regions of the medical image. Second, the watermarked dataset is created by embedding watermarks within a subset of target class samples and combining them with the remaining dataset. Finally, black-box dataset ownership verification is performed using hypothesis testing to detect whether watermarked, non-target class samples were misclassified by the suspicious model.

picious model will behave normally on benign samples but misclassify the watermarked samples.

3.2 Proposed Method

As described in previous sections, existing DOV methods designed for natural images are incompatible with the constraints imposed by medical imaging. To overcome these limitations and ensure watermark stealthiness and robustness, we propose X-Mark, a sample-specific clean-label backdoor watermarking method for medical image copyright protection. Our work builds upon recent advances in clean-label backdoor watermarking, where a self-supervised, specialized watermark generator is used to embed watermark samples into the benign dataset [Wang *et al.*, 2025]. We condition the watermark generator to produce perturbations within salient regions, and introduce Laplacian regularization to achieve watermark scale-invariance. As shown in Figure 1, our method consists of three steps: (1) Training the conditional scale-invariant watermark generator, (2) Dataset watermarking, and (3) Dataset ownership verification.

Conditional Scale-Invariant Watermark Generator The goal of the watermark generator is to ensure that a suspicious model $f_w(\cdot; \omega)$ would learn the association between watermarked sample and the presence of target label k . Specifically, the suspicious model $f_w(\cdot; \omega)$ should trigger the backdoor when watermark signal (*i.e.*, perturbations) present and cause misclassifications to $y_t^{(k)}$. This presents a dual objective that the samples produced by the watermark generator $G(\cdot; \theta)$ must simultaneously satisfy in the clean-label setting:

Objective I. During dataset watermarking, only samples from the target class are watermarked in the released dataset. The watermark generator should produce watermarked samples from the target class containing perturbations that reinforce the watermark-label association, such that when these

samples would be misclassified by a suspicious classifier $f_w(\cdot; \omega)$.

$$f_w(G(\mathbf{x}_{t,i}; \theta); \omega)^{(k)} = 0 \quad (1)$$

Objective II. During DOV, only samples from the non-target class are used for verification. The watermark generator should produce watermarked samples from the non-target class such that the suspicious classifier $f_w(\cdot; \omega)$ would misclassify them as $y_t^{(k)}$.

$$f_w(G(\mathbf{x}_{nt,i}; \theta); \omega)^{(k)} = 1 \quad (2)$$

We use a conditional U-Net autoencoder as our watermark generator $G(\cdot; \theta)$. Unlike SSCL-BW [Wang *et al.*, 2025], which used the original U-Net architecture [Ronneberger *et al.*, 2015], our model adopts a residual U-Net with strided convolutions to improve computational efficiency at higher image resolutions. This reduces parameter count by 25% and MAC operations by 72% compared to the original U-Net. Additionally, we incorporate an EigenCAM-based [Muhammad and Yeasin, 2020] saliency conditioning module at the bottleneck via convolutional projection to condition the generator to produce perturbations within salient regions of the sample. We choose EigenCAM over other gradient-based activation maps (*e.g.*, Grad-CAM) for its efficiency.

To train the watermark generator $G(\cdot; \theta)$ such that watermarked samples satisfy the dual objective and medical imaging constraint, we use a surrogate benign classifier $f(\cdot; \omega)$ and training objective consisting of four components: (1) Target sample loss \mathcal{L}_t , (2) Non-target sample loss \mathcal{L}_{nt} , (3) Perceptual similarity loss \mathcal{L}_{LPIPS} and (4) Laplacian pyramid loss \mathcal{L}_{Lap} . While the first three components are inspired by prior work [Wang *et al.*, 2025], we introduce \mathcal{L}_{Lap} to regularize the watermark generator by penalizing high-frequency perturbations and mitigating strong, unrealistic perturbations, encouraging the model to produce perturbations that are robust to

downsampling. The overall training objective is the weighted average of all four components:

$$\mathcal{L} = \lambda_t \mathcal{L}_t + \lambda_{nt} \mathcal{L}_{nt} + \lambda_{\text{LPIPS}} \mathcal{L}_{\text{LPIPS}} + \lambda_{\text{Lap}} \mathcal{L}_{\text{Lap}} \quad (3)$$

where $\lambda_t = \lambda_{nt} = 1$, $\lambda_{\text{Lap}} = 3$, and $\lambda_{\text{LPIPS}} = 10$.

The target sample loss \mathcal{L}_t measures the loss of the surrogate model on watermarked samples from the target class:

$$\mathcal{L}_t = \mathbb{E}_{\mathbf{x}_t \sim \mathcal{D}_t} \mathcal{H}_b(f(G(\mathbf{x}_t; \theta); \omega)^{(k)}, 0) \quad (4)$$

where \mathcal{H}_b is binary cross-entropy (BCE) loss, $\mathcal{D}_t \subset \mathcal{D}$ is the set of target samples.

Similarly, the non-target sample loss \mathcal{L}_{nt} measures the loss of the surrogate model on watermarked samples from the non-target class:

$$\mathcal{L}_{nt} = \mathbb{E}_{\mathbf{x}_{nt} \sim \mathcal{D}_{nt}} \mathcal{H}_b(f(G(\mathbf{x}_{nt}; \theta); \omega)^{(k)}, 1) \quad (5)$$

where $\mathcal{D}_{nt} \subset \mathcal{D}$ is the set of non-target samples.

To ensure watermark imperceptibility and preserve diagnostic quality, the LPIPS metric measures the perceptual similarity between benign and watermarked samples from both target and non-target classes [Zhang *et al.*, 2018]:

$$\mathcal{L}_{\text{LPIPS}} = \mathbb{E}_{\mathbf{x} \sim \mathcal{D}} \text{LPIPS}(G(\mathbf{x}; \theta), \mathbf{x}) \quad (6)$$

To achieve watermark scale-invariance, we incorporate Laplacian regularization using the Laplacian pyramid loss \mathcal{L}_{Lap} to penalizes differences across multiple frequency levels [Denton *et al.*, 2015; Bojanowski *et al.*, 2017]:

$$\mathcal{L}_{\text{Lap}} = \sum_{l=1}^L \mathbb{E}_{\mathbf{x} \sim \mathcal{D}} \|\mathcal{L}^{(l)}(G(\mathbf{x}; \theta)) - \mathcal{L}^{(l)}(\mathbf{x})\|_1 \quad (7)$$

where $\mathcal{L}^{(l)}$ is the l -th level of the Laplacian pyramid decomposition and $L = 3$ is the number of pyramid levels.

We constraint the perturbation between the benign sample \mathbf{x}_i and its watermarked version $\hat{\mathbf{x}}_i$ by the budget ϵ :

$$\|G(\mathbf{x}_i; \theta) - \mathbf{x}_i\|_\infty \leq \epsilon \quad (8)$$

Following prior work, we set $\epsilon = 16/255$ [Li *et al.*, 2022].

Dataset Watermarking We embed watermarked samples into the benign dataset following prior clean-label backdoor watermarks [Li *et al.*, 2022]. We select a subset $\mathcal{D}_s \subset \mathcal{D}$ of benign samples from the target class with watermarking rate γ . For each sample $\mathbf{x}_{t,i}$, we generate its watermarked version $\hat{\mathbf{x}}_{t,i}$ using the watermark generator $G(\cdot; \theta)$. These watermarked samples are then merged with the remaining dataset $\mathcal{D} \setminus \mathcal{D}_s$ to create the watermarked dataset \mathcal{D}_w , and is subsequently released for legitimate use. The goal is that a suspicious model trained on the watermarked dataset would inherit the watermark-label association and trigger the backdoor upon verification. Furthermore, our watermarks are hard to detect with manual inspection due to the sample-specific clean-label nature of our method.

Dataset Ownership Verification Suppose an unauthorized user fine-tunes a pre-trained model $f(\cdot; \omega)$ on the watermarked dataset \mathcal{D}_w , resulting in the backdoored model $f_w(\cdot; \omega)$. Given this suspicious model in black-box setting, we follow prior clean-label backdoor watermarks for

probability-available verification [Li *et al.*, 2022]. Specifically, if the model was trained on the watermarked dataset \mathcal{D}_w , the watermark should trigger the backdoor and verification samples would be misclassified as $y_t^{(k)} = 1$. To prevent selection bias, probability-available verification uses a hypothesis-test to check if the posterior probability for the target class of benign samples is significantly lower than that of their watermarked versions.

Formally, let \mathcal{X} denote the set of benign samples from the non-target class, and $\mathcal{X}' = G(\mathcal{X}; \theta)$ be their watermarked versions. Let $P_b = f_w(\mathcal{X})^{(k)}$ and $P_v = f_w(\mathcal{X}')^{(k)}$ denote the posterior probabilities of \mathcal{X} and \mathcal{X}' on the target class $y_t^{(k)}$ respectively. Consider the null hypothesis:

$$H_0 : P_b + \tau = P_v \quad (9)$$

$$H_1 : P_b + \tau < P_v \quad (10)$$

where $\tau \in [0, 1]$ is the accepted margin. If the resulting p-value of one-sided paired t-test is significant, H_0 is rejected and we conclude that the suspicious model was trained on the watermarked dataset \mathcal{D}_w . Additionally, we compute the confidence score $\Delta P = P_b - P_v$, where a larger ΔP indicates higher verification effectiveness. Statistical significance is defined as $p < 0.05$.

4 Experiments

4.1 Experimental Setup

Dataset We conduct experiments on CheXpert [Irvin *et al.*, 2019], containing $n = 224,316$ frontal and lateral CXRs from 65,240 patients annotated for the presence of 14 radiological findings. Specifically, we focus on the six CheXpert-defined competition labels: Atelectasis, Cardiomegaly, Consolidation, Edema, and Pleural Effusion as well as No Finding, which represents the absence of any pathology.

Implementation We train the surrogate model $f(\cdot; \omega)$ on the benign dataset using an ImageNet pre-trained ResNet18 for 5 epochs with AdamW optimizer, batch size of 32, and learning rate of 1e-4 at the resolution of 224×224 . To train the watermark generator $G(\cdot; \theta)$, we select 10% of samples from the target class and an equal number of samples from the non-target class to ensure a balanced training set. During generator training, we compute EigenCAMs from the final convolutional layer of the surrogate model and use them as conditioning input to guide perturbations towards salient regions. The generator is optimized using AdamW with a batch size of 32 and learning rate of 1e-4 for up to 100 epochs at resolution 1024×1024 . Finally, the backdoored model $f_w(\cdot; \omega)$ is trained similarly to the surrogate model using an ImageNet pre-trained ResNet18 for 5 epochs with AdamW optimizer, batch size of 32, and learning rate of 1e-4 at the resolution of 224×224 . All models are implemented in PyTorch and trained with random augmentations, mixed-precision, and 8 NVIDIA L40S GPUs on a shared HPC.

Evaluation Metrics We measure the performance of our watermarking method across dataset watermarking and DOV tasks. For dataset watermarking, we evaluate watermark effectiveness and imperceptibility using benign accuracy (BA),

Table 1: Benign accuracy (%), watermark success rate (%), and perceptual similarity of dataset watermarking on CheXpert.

Type↓	Method↓, Metric→	BA (%)	WSR (%)	LPIPS
Benign	No Attack	81.89	-	-
Poison-Label	BadNets [Gu <i>et al.</i> , 2017]	80.69	100	0.009
	Blended [Chen <i>et al.</i> , 2017]	83.23	97.31	0.003
	WaNet [Nguyen and Tran, 2021]	82.48	16.81	0.004
	UBW-P [Li <i>et al.</i> , 2022]	84.28	22.45	0.009
Clean-Label	Label-Consistent [Turner <i>et al.</i> , 2019]	80.69	100	0.009
	SSCL-BW [Wang <i>et al.</i> , 2025]	82.93	100	0.023
	X-Mark (Ours)	84.88	100	0.020

Table 2: Effectiveness (ΔP and p-value) of probability-available dataset ownership verification on CheXpert.

Method↓	Metric↓, Scenario→	Ind-W	Ind-M	Malicious
SSCL-BW [Wang <i>et al.</i> , 2025]	ΔP	-0.0004	0.2925	0.8705
	p-value	1.0	0.0580	10^{-60}
X-Mark (Ours)	ΔP	-0.0005	0.2564	0.8378
	p-value	1.0	0.4102	10^{-53}

watermark success rate (WSR) and perceptual similarity (LPIPS). Briefly, BA measures the accuracy of benign samples being correctly classified, while WSR measures the proportion of non-target watermarked samples that are misclassified as the target-class by the suspicious model. While AUROC is primarily used as the evaluation metric in medical image classification, we compute the optimal F1 threshold on the validation set and calculate accuracy on the test set to maintain consistency with prior works. For DOV, we evaluate verification effectiveness using confidence $\Delta P \in [-1, 1]$ and p-value $p \in [0, 1]$. A larger ΔP and smaller p indicates a high likelihood that the suspicious model was trained on the watermarked dataset.

4.2 Performance of Dataset Watermarking

Setting We evaluate the effectiveness and imperceptibility by comparing our method with existing backdoor watermarking methods. For the poison-label setting, we include BadNets [Gu *et al.*, 2017], Blended attack [Chen *et al.*, 2017], WaNet [Nguyen and Tran, 2021], and UBW-P [Li *et al.*, 2022] as baselines. For the clean-label setting, we include Label-Consistent [Turner *et al.*, 2019] and SSCL-BW [Wang *et al.*, 2025] as baselines. Additionally, we include the “No Attack” scenario as our BA reference. The target label is set as “No Finding” and watermarking rate is set as $\gamma = 0.1$.

Results As shown in Table 1, our method demonstrates strong watermark effectiveness while maintaining imperceptibility, achieving highest BA of 84.88% and WSR of 100%. Among the poison-label baselines, BadNets and Blended attacks achieve high WSRs (100% and 97.31%). However, they rely on static trigger patterns that need to be large enough to survive downsampling, making them easily detectable. WaNet watermarks fail to survive downsampling, only achieving a WSR of 16.81%. Similarly, UBW-P with a WSR of 22.45% scales poorly to the multi-label setting due to its untargeted nature. In the clean-label setting, Label-Consistent and SSCL-BW both reach WSR of 100%. Label-Consistent relies on static triggers, while SSCL-BW generates strong perturbations (LPIPS of 0.023) that produce unrealistic anatomy,

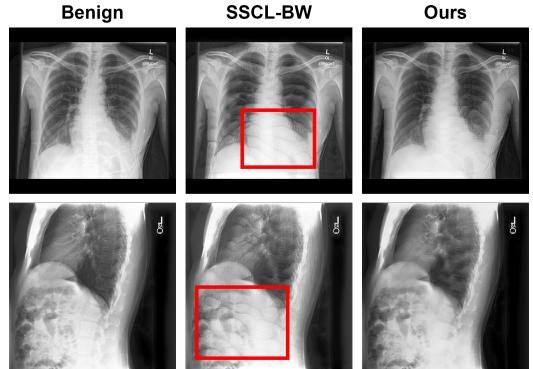


Figure 2: Example watermarked samples from SSCL-BW and X-Mark. Red box indicates region of strong perturbations, resulting in anatomically improbable structures that are easy to detect upon manual inspection. Saliency conditioning limits perturbations within salient regions (chest) while Laplacian regularization mitigates strong, unrealistic perturbations.

as shown in Figure 2. Results indicate that CXR datasets are well-suited for dataset watermarking, likely due to their limited visual diversity compared to natural images, allowing perturbations to remain in-distribution and exploit short-cut learning [Jabbour *et al.*, 2020].

4.3 Performance of Dataset Ownership Verification

Setting Following prior work [Li *et al.*, 2022; Li *et al.*, 2023], we evaluate the effectiveness of probability-available verification across three scenarios: (1) Independent Watermark (Ind-W), where the suspicious model trained on the watermarked dataset is queried with a different watermark than that produced by our method. (2) Independent Model (Ind-M), where a suspicious benign model is queried with the watermarks produced by our method. (3) Malicious, where the suspicious model trained on the watermarked dataset is queried with the watermarks produced by our method. Addi-

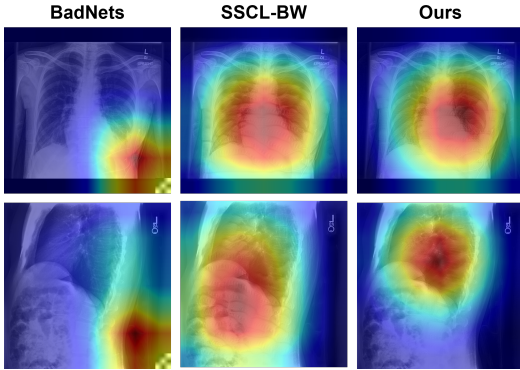


Figure 3: Watermarked samples and their EigenCAM-based saliency maps from backdoored models using BadNets, SSCL-BW, and X-Mark. For BadNets, the EigenCAM mainly focuses on the trigger, while focusing on regions with the largest perturbations in SSCL-BW. In contrast, in our method, the EigenCAM focuses on the salient regions (i.e., the chest), making the backdoor difficult to detect even with automated methods.

tionally, we also report the verification effectiveness of the SSCL-BW [Wang *et al.*, 2025] as it is our primary baseline. We randomly sample $n = 100$ benign samples from the dataset and set $\tau = 0.25$ for the hypothesis test.

Results As shown in Table 2, our method demonstrates effective verification in the probability-available black-box setting. It accurately detects whether the suspicious model $f_w(\cdot; \omega)$ was trained on the watermarked dataset \mathcal{D}_w in the “Malicious” scenario, achieving $\Delta P > 0.8$ and $p < 0.001$. It also does not produce false positives in the “Ind-W” scenario, where $\Delta P \approx 0$ and $p = 1.0$. However, in the “Ind-M” scenario, we observe $\Delta P = 0.26$ and $p = 0.41$, indicating a greater probability of false positives for benign models. While SSCL-BW exhibits comparable performance in the “Malicious” and “Ind-W” scenarios, its performance in “Ind-M” is substantially worse with $p = 0.06$. We attribute this behavior to the challenges discussed previously in medical imaging. It is likely that watermark perturbations are in-domain to the feature representation naturally learned by classifier, causing benign models to also exhibit backdoored behavior. A potential solution may involve injecting out-of-distribution perturbations [Guo *et al.*, 2024; Feng *et al.*, 2022].

4.4 Transferability of X-Mark

We explore the transferability and robustness of our watermarking method across two settings: (1) Watermark scale-invariance, and (2) Model-agnostic transferability.

Watermark Scale-Invariance We train backdoored models $f_w(\cdot; \omega)$ on the watermarked dataset \mathcal{D}_w at resolutions of 32×32 , 64×64 , 128×128 , 224×224 , 256×256 , 512×512 and 1024×1024 , using the same settings described previously. All images are resized to the target resolution using bilinear interpolation while preserving aspect ratio via zero-padding. As shown in Figure 4, the backdoored models inherit the watermark-label association even when images are downsampled. We observe that consistent BA and WSR up

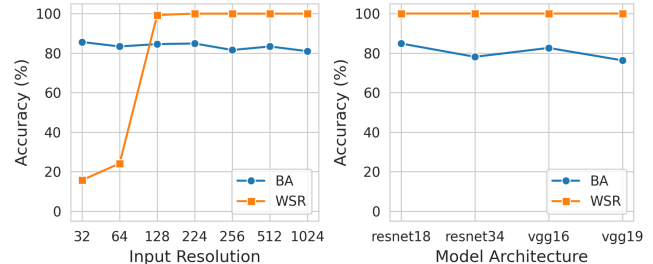


Figure 4: Transferability of X-Mark, demonstrating watermark scale-invariance and model-agnostic transferability.

to 128×128 resolution. However, watermark effectiveness decreases when the resolution is further reduced to 64×64 and 32×32 . This demonstrates that the watermark generator produces perturbations that are robust to downsampling and remain scale-invariant up to a certain resolution.

Model-Agnostic Transferability We train backdoored models $f_w(\cdot; \omega)$ using the watermarked dataset \mathcal{D}_w using four distinct architectures: ResNet18, ResNet34, VGG16-BN, and VGG19-BN. All models are trained using the same settings described previously. As shown in Figure 4, all architectures inherit the backdoor behavior, consistently reaching a WSR of 100%. This indicates that the watermarked samples are model-agnostic and retain their effectiveness across different model architectures.

4.5 Ablation Study

We explore dataset watermarking performance of our method under various settings, specifically the impact of the proposed components (saliency conditioning and Laplacian regularization) and core hyperparameters (watermarking rate γ and perturbation budget ϵ). All experiments are conducted under the same settings described previously.

Impact of Saliency Conditioning To study the impact of saliency conditioning, we train watermark generators $G(\cdot; \theta)$ with and without the EigenCAM-based saliency conditioning module. As shown in Table 3, dataset watermarking performance is not affected by saliency conditioning, with comparable BA, WSR, and LPIPS metrics across both settings. We observe a decrease in \mathcal{L}_{Lap} even when Laplacian regularization is not applied, likely due to the perturbations being concentrated within salient regions of the image. This behavior is visualized in Figure 5.

Impact of Laplacian Regularization To study the impact of Laplacian regularization, we train watermark generators $G(\cdot; \theta)$ with and without the Laplacian pyramid loss \mathcal{L}_{Lap} in the training objective. As shown in Table 3, we observe an increase in BA ($\sim 4\%$) and decrease in \mathcal{L}_{Lap} , while WSR and LPIPS remain unchanged. This indicates that Laplacian regularization mitigates high-frequency perturbations. We visualize the high-frequency information using the Laplacian filter ∇^2 (i.e., high-pass filter) in Figure 5.

Impact of Watermarking Rate To study the impact of watermarking rate γ , we train backdoored models $f_w(\cdot; \omega)$ with γ ranging from 0.1% to 10%. As shown in Figure 6, even

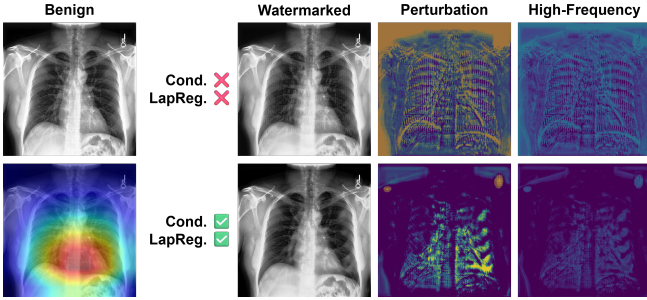


Figure 5: An example illustrating the impact of EigenCAM-based saliency conditioning and Laplacian regularization.

Table 3: Impact of EigenCAM-based saliency conditioning and Laplacian regularization of dataset watermarking performance on CheXpert.

Cond.	LapReg.	BA (%)	WSR (%)	LPIPS	\mathcal{L}_{Lap}
✗	✗	80.24	100	0.019	0.042
✗	✓	84.58	100	0.019	0.014
✓	✗	80.39	100	0.020	0.019
✓	✓	84.88	100	0.020	0.013

at a low rate of $\gamma = 1\%$, the WSR reaches 100% while BA is unaffected. This indicates that increasing γ improves watermark effectiveness without impacting model performance on benign samples. The high WSR observed at very low $\gamma = 0.01\%$ can be attributed to the sensitivity of benign models to the watermark, consistent with the observations made in the “Ind-M” scenario.

Impact of Perturbation Budget To study the impact of perturbation budget ϵ , we train watermark generators $G(\cdot; \theta)$ with ϵ ranging from 2/255 to 16/255. As shown in Figure 6, increasing ϵ leads to higher WSR, while BA remains comparable across all settings. Even at a budget of $\epsilon = 6/255$, the WSR reaches 100%, demonstrating that effective watermarks can be achieved with relatively small perturbations. However, larger values of ϵ involve a trade-off with imperceptibility, as larger perturbations in watermarked samples would be evident upon manual inspection.

4.6 Resistance to Adaptive Attacks

We explore whether our method is resistant to existing backdoor defenses that an unauthorized user may employ to avoid detection. Using the same settings as previously described, we focus on two representative watermark removal attacks: (1) Model fine-tuning [Liu *et al.*, 2017] and (2) Model pruning [Liu *et al.*, 2018].

Model Fine-tuning We randomly select 10% of benign samples from the dataset to fine-tune the backdoored model $f_w(\cdot : \omega)$ for up to 100 epochs. Specifically, only the fully-connected layers of $f_w(\cdot : \omega)$ are fine-tuned while convolutional layers are frozen. As shown in Figure 7, both BA and WSR generally remain consistent even after fine-tuning for 100 epochs. This indicates that model fine-tuning has little-to-no impact on watermark performance.

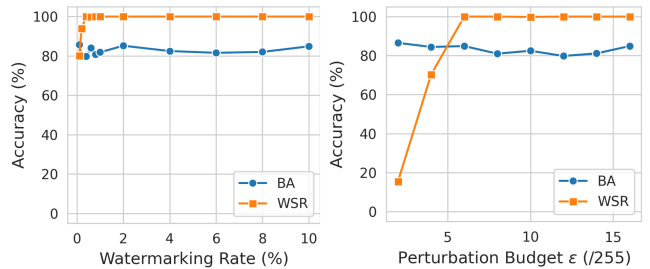


Figure 6: Impact of γ and ϵ on X-Mark dataset watermarking.

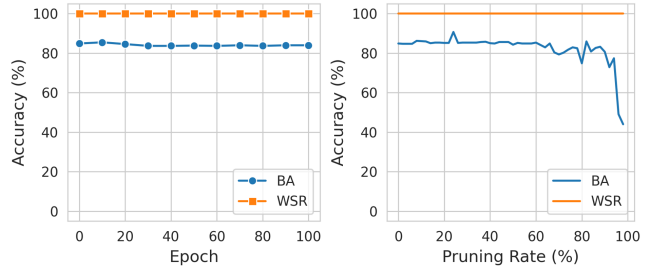


Figure 7: Resistance of X-Mark to model fine-tuning and pruning.

Model Pruning We randomly select 10% of benign samples from the dataset to prune the latent representation of the backdoored model $f_w(\cdot : \omega)$ with a pruning rate $\beta \in \{0, 0.02, \dots, 0.98\}$. Specifically, we use fine-pruning [Liu *et al.*, 2018] on the output of the last convolutional layer. As shown in Figure 7, BA gradually decreases as pruning rate increases, while WSR remains unchanged across all rates. We attribute high WSR at high pruning rates due to watermarked samples consistently having higher prediction probabilities than benign samples, resulting in WSR of 100%.

5 Conclusion

In this paper, we propose X-Mark, a sample-specific clean-label backdoor watermarking method for copyright protection of CXR datasets. Our method addresses the challenges presented by CXRs, namely, the dynamic and high-resolution of scans, limited visual diversity, and need for preserving diagnostic quality. We use a U-Net watermark generator with an EigenCAM-based saliency conditioning module that embeds unique perturbations within salient regions of the CXR. Additionally, we introduce Laplacian regularization to penalize high-frequency perturbations and prevent strong, unrealistic perturbations, allowing the watermark to survive down-sampling and be visually indistinguishable from benign samples. Experimental results on CheXpert show that X-Mark outperforms existing clean-label watermarking methods in effectiveness, imperceptibility, transferability, and resilience against watermark removal attacks. More importantly, it demonstrates robustness under medical imaging settings. Future work will explore extending our method to other medical imaging tasks (particularly, segmentation) and applications in medical VLMs.

References

[Abadi *et al.*, 2016] Martin Abadi, Andy Chu, Ian Goodfellow, H Brendan McMahan, Ilya Mironov, Kunal Talwar, and Li Zhang. Deep learning with differential privacy. In *ACM SIGSAC Conference on Computer and Communications Security*, pages 308–318, 2016.

[Adi *et al.*, 2018] Yossi Adi, Carsten Baum, Moustapha Cisse, Benny Pinkas, and Joseph Keshet. Turning your weakness into a strength: Watermarking deep neural networks by backdooring. In *27th USENIX Security Symposium*, pages 1615–1631, 2018.

[Bojanowski *et al.*, 2017] Piotr Bojanowski, Armand Joulin, David Lopez-Paz, and Arthur Szlam. Optimizing the latent space of generative networks. *arXiv preprint arXiv:1707.05776*, 2017.

[Chen *et al.*, 2017] Xinyun Chen, Chang Liu, Bo Li, Kimberly Lu, and Dawn Song. Targeted backdoor attacks on deep learning systems using data poisoning. *arXiv preprint arXiv:1712.05526*, 2017.

[Cong *et al.*, 2022] Tianshuo Cong, Xinlei He, and Yang Zhang. Sslguard: A watermarking scheme for self-supervised learning pre-trained encoders. In *ACM SIGSAC Conference on Computer and Communications Security*, pages 579–593, 2022.

[Denton *et al.*, 2015] Emily L Denton, Soumith Chintala, Rob Fergus, et al. Deep generative image models using a laplacian pyramid of adversarial networks. *Advances in neural information processing systems*, 28, 2015.

[Diaz-Pinto *et al.*, 2024] Andres Diaz-Pinto, Sachidanand Alle, Vishwesh Nath, Yucheng Tang, Alvin Ihsani, Muhammad Asad, Fernando Pérez-García, Pritesh Mehta, Wenqi Li, Mona Flores, et al. Monai label: A framework for ai-assisted interactive labeling of 3d medical images. *Medical Image Analysis*, 95:103207, 2024.

[Ebrahimian *et al.*, 2022] Shadi Ebrahimian, Mannudeep K Kalra, Sheela Agarwal, Bernardo C Bizzo, Mona Elkholby, Christoph Wald, Bibb Allen, and Keith J Dreyer. Fda-regulated ai algorithms: trends, strengths, and gaps of validation studies. *Academic radiology*, 29(4):559–566, 2022.

[Feng *et al.*, 2022] Yu Feng, Benteng Ma, Jing Zhang, Shanshan Zhao, Yong Xia, and Dacheng Tao. Fibaf: Frequency-injection based backdoor attack in medical image analysis. In *Proceedings of the IEEE/CVF Conference on Computer Vision and Pattern Recognition*, pages 20876–20885, 2022.

[Gu *et al.*, 2017] Tianyu Gu, Brendan Dolan-Gavitt, and Siddharth Garg. Badnets: Identifying vulnerabilities in the machine learning model supply chain. In *Neural Information Processing Systems Workshop on Machine Learning Security*, 2017.

[Guo *et al.*, 2024] Junfeng Guo, Yiming Li, Lixu Wang, Shu-Tao Xia, Heng Huang, Cong Liu, and Bo Li. Domain watermark: Effective and harmless dataset copyright protection is closed at hand. In *Advances in Neural Information Processing Systems*, volume 36, 2024.

[Hua *et al.*, 2023] Guang Hua, Andrew Beng Jin Teoh, Yong Xiang, and Hao Jiang. Unambiguous and high-fidelity backdoor watermarking for deep neural networks. *IEEE Transactions on Neural Networks and Learning Systems*, 35(8):11204–11217, 2023.

[Huang *et al.*, 2021] Hanxun Huang, Xingjun Ma, Sarah Monazam Erfani, James Bailey, and Yisen Wang. Unlearnable examples: Making personal data unexploitable. In *International Conference on Learning Representations*, 2021.

[Irvin *et al.*, 2019] Jeremy Irvin, Pranav Rajpurkar, Michael Ko, Yifan Yu, Silviana Ciurea-Ilcus, Chris Chute, Henrik Marklund, Behzad Haghgoo, Robyn Ball, Katie Shpanskaya, et al. CheXpert: A large chest radiograph dataset with uncertainty labels and expert comparison. In *Proceedings of the AAAI conference on artificial intelligence*, volume 33, pages 590–597, 2019.

[Jabbour *et al.*, 2020] Sarah Jabbour, David Fouhey, Ella Kazerooni, Michael W Sjoding, and Jenna Wiens. Deep learning applied to chest x-rays: exploiting and preventing shortcuts. In *Machine Learning for Healthcare Conference*, pages 750–782. PMLR, 2020.

[Johnson *et al.*, 2019] Alistair EW Johnson, Tom J Pollard, Seth J Berkowitz, Nathaniel R Greenbaum, Matthew P Lungren, Chih-ying Deng, Roger G Mark, and Steven Horng. Mimic-cxr, a de-identified publicly available database of chest radiographs with free-text reports. *Scientific data*, 6(1):317, 2019.

[Johnson *et al.*, 2023] Alistair EW Johnson, Lucas Bulgarelli, Lu Shen, Alvin Gayles, Ayad Shammout, Steven Horng, Tom J Pollard, Sicheng Hao, Benjamin Moody, Brian Gow, et al. Mimic-iv, a freely accessible electronic health record dataset. *Scientific data*, 10(1):1, 2023.

[Kancharla and others, 2024] Pranay Kancharla et al. Medical image data provenance for medical cyber-physical system. *arXiv preprint arXiv:2403.15522*, 2024.

[Li *et al.*, 2022] Yiming Li, Yang Bai, Yong Jiang, Yong Yang, Shu-Tao Xia, and Bo Li. Untargeted backdoor watermark: Towards harmless and stealthy dataset copyright protection. In *Advances in Neural Information Processing Systems*, volume 35, pages 13238–13250, 2022.

[Li *et al.*, 2023] Yiming Li, Mingyan Zhu, Xue Yang, Yong Jiang, Tao Wei, and Shu-Tao Xia. Black-box dataset ownership verification via backdoor watermarking. *IEEE Transactions on Information Forensics and Security*, 18:2318–2332, 2023.

[Liu *et al.*, 2017] Yuntao Liu, Yang Xie, and Ankur Srivastava. Neural trojans. In *2017 IEEE international conference on computer design (ICCD)*, pages 45–48. IEEE, 2017.

[Liu *et al.*, 2018] Kang Liu, Brendan Dolan-Gavitt, and Siddharth Garg. Fine-pruning: Defending against backdooring attacks on deep neural networks. In *International symposium on research in attacks, intrusions, and defenses*, pages 273–294. Springer, 2018.

[Ma *et al.*, 2024] Jun Ma, Yuting He, Feifei Li, Lin Han, Chenyu You, and Bo Wang. Segment anything in medical images. *Nature Communications*, 15(1):654, 2024.

[Maini *et al.*, 2021] Pratyush Maini, Mohammad Yaghini, and Nicolas Papernot. Dataset inference: Ownership resolution in machine learning. In *International Conference on Learning Representations*, 2021.

[Muhammad and Yeasin, 2020] Mohammed Bany Muhammad and Mohammed Yeasin. Eigen-cam: Class activation map using principal components. In *2020 international joint conference on neural networks (IJCNN)*, pages 1–7. IEEE, 2020.

[Nguyen and Tran, 2021] Anh Nguyen and Anh Tran. Wanet-imperceptible warping-based backdoor attack. *arXiv preprint arXiv:2102.10369*, 2021.

[Poonam and Arora, 2022] Poonam and Sumit Arora. Advances in medical image watermarking: a state of the art review. *Multimedia Tools and Applications*, 81:1–35, 2022.

[Rajpurkar and Lungren, 2023] Pranav Rajpurkar and Matthew P Lungren. The current and future state of ai interpretation of medical images. *New England Journal of Medicine*, 388(21):1981–1990, 2023.

[Ronneberger *et al.*, 2015] Olaf Ronneberger, Philipp Fischer, and Thomas Brox. U-net: Convolutional networks for biomedical image segmentation. In *International Conference on Medical image computing and computer-assisted intervention*, pages 234–241. Springer, 2015.

[Sablayrolles *et al.*, 2020] Alexandre Sablayrolles, Matthijs Douze, Cordelia Schmid, and Hervé Jégou. Radioactive data: tracing through training. In *International Conference on Machine Learning*, pages 8326–8335, 2020.

[Senbekov *et al.*, 2020] Meiram Senbekov, Timur Saliev, Zarina Bukeyeva, Aigul Almabayeva, Murat Zhanaliyeva, Nurgul Aitenova, Yerzhan Toishibekov, Ildar Fakhradiyev, et al. The recent progress and applications of digital technologies in healthcare: a review. *International Journal of Telemedicine and Applications*, 2020, 2020.

[Shao *et al.*, 2025] Shuo Shao, Yiming Li, Mengren Zheng, Zhiyang Hu, Yukun Chen, Boheng Li, Yu He, Junfeng Guo, Dacheng Tao, and Zhan Qin. Databench: Evaluating dataset auditing in deep learning from an adversarial perspective. *arXiv preprint arXiv:2507.05622*, 2025.

[Sun and others, 2024] Weixiang Sun et al. Medical unlearnable examples: Securing medical data from unauthorized training via sparsity-aware local masking. *arXiv preprint arXiv:2403.10573*, 2024.

[Tang *et al.*, 2023] Ruixiang Tang, Qizhang Feng, Ninghao Liu, Fan Yang, and Xia Hu. Did you train on my dataset? towards public dataset protection with cleanlabel backdoor watermarking. *ACM SIGKDD Explorations Newsletter*, 25(1):43–53, 2023.

[Turner *et al.*, 2019] Alexander Turner, Dimitris Tsipras, and Aleksander Madry. Label-consistent backdoor attacks. *arXiv preprint arXiv:1912.02771*, 2019.

[Wang *et al.*, 2025] Yingjia Wang, Ting Qiao, Xing Liu, Chongzuo Li, Sixing Wu, and Jianbin Li. Ssclbw: Sample-specific clean-label backdoor watermarking for dataset ownership verification. *arXiv preprint arXiv:2510.26420*, 2025.

[Wu *et al.*, 2022] Yutong Wu, Han Qiu, Tianwei Zhang, and Meikang Qiu. Watermarking pre-trained encoders in contrastive learning. In *International Conference on Machine Learning*, 2022.

[Zhang *et al.*, 2018] Richard Zhang, Phillip Isola, Alexei A Efros, Eli Shechtman, and Oliver Wang. The unreasonable effectiveness of deep features as a perceptual metric. In *Proceedings of the IEEE conference on computer vision and pattern recognition*, pages 586–595, 2018.

[Zhu *et al.*, 2025] Hongyu Zhu, Sichu Liang, Wenwen Wang, Zhuomeng Zhang, Fangqi Li, and Shi-Lin Wang. Evading data provenance in deep neural networks. In *IEEE/CVF International Conference on Computer Vision*, pages 1249–1260, 2025.